

Article

An Explicit Fourth-Order Compact Numerical Scheme for Heat Transfer of Boundary Layer Flow

Yasir Nawaz ¹, Muhammad Shoab Arif ¹ , Wasfi Shatanawi ^{2,3,4,*}  and Amna Nazeer ⁵

¹ Department of Mathematics, Air University Islamabad, PAF Complex E-9, Islamabad Capital Territory 44000, Pakistan; yasir_maths@yahoo.com (Y.N.); shoab.arif@mail.au.edu.pk (M.S.A.)

² Department of Mathematics and General Sciences, Prince Sultan University Riyadh, Riyadh 12435, Saudi Arabia

³ Department of Medical Research, China Medical University Hospital, China Medical University, Taichung 40402, Taiwan

⁴ Department of Mathematics, Hashemite University, Zarqa 13115, Jordan

⁵ Department of Mathematics, Comsats University, Islamabad Capital Territory 45550, Pakistan; amna.nazeer@comsats.edu.pk

* Correspondence: wshatanawi@psu.edu.sa

Abstract: The main contribution of this article is to propose a compact explicit scheme for solving time-dependent partial differential equations (PDEs). The proposed explicit scheme has an advantage over the corresponding implicit compact scheme to find solutions of nonlinear and linear convection–diffusion type equations because the implicit existing compact scheme fails to obtain the solution. In addition, the present scheme provides fourth-order accuracy in space and second-order accuracy in time, and is constructed on three grid points and three time levels. It is a compact multistep scheme and conditionally stable, while the existing multistep scheme developed on three time levels is unconditionally unstable for parabolic and considered a type of equations. The mathematical model of the heat transfer in a mixed convective radiative fluid flow over a flat plate is also given. The convergence conditions of dimensionless forms of these equations are given, and also the proposed scheme solves equations, and results are compared with two existing schemes. It is hoped that the results in the current report are a helpful source for future fluid-flow studies in an industrial environment in an enclosure area.

Keywords: compact explicit scheme; nonlinear PDEs; flow over the plate; mixed convection; thermal radiation



Citation: Nawaz, Y.; Arif, M.S.; Shatanawi, W.; Nazeer, A. An Explicit Fourth-Order Compact Numerical Scheme for Heat Transfer of Boundary Layer Flow. *Energies* **2021**, *14*, 3396. <https://doi.org/10.3390/en14123396>

Academic Editors: Magdalena Piasecka and Krzysztof Dutkowski

Received: 9 May 2021

Accepted: 2 June 2021

Published: 9 June 2021

Publisher's Note: MDPI stays neutral with regard to jurisdictional claims in published maps and institutional affiliations.



Copyright: © 2021 by the authors. Licensee MDPI, Basel, Switzerland. This article is an open access article distributed under the terms and conditions of the Creative Commons Attribution (CC BY) license (<https://creativecommons.org/licenses/by/4.0/>).

1. Introduction

The linear reaction convection diffusion equation has a broad range of application in astrophysics, aerospace sciences, biology, and environmental sciences. Energy movements [1,2], fluid clotting [3], and hemodynamics [4] are the areas with relevance to the convection–diffusion equation. The Black–Scholes equation [5,6] is a practical equation for options pricing, transformed into a reaction–convection–diffusion equation on a semi-unbounded domain [7,8].

The mathematical conversion of a linear reaction convection–diffusion equation into a nonstandard finite difference equation was revealed by [9]; however, [10] proposed a study that comprised the family of positivity-preserving finite-difference methods for the classical Fisher–Kolmogorov–Petrovsky–Piscounov equation.

The fourth-order compact finite difference scheme was studied by Sun and Zhang [11] using parameters such as space and time. Additionally, when $\alpha = 0$ & $\alpha \neq 0$, Mohebbi and Dehghan [12] offered some compact methods that suggested a fourth-order compact finite difference in space and time components for Equation (A1). Moreover, Nove [13] studied a three-point third-order implicit finite difference method that is conditionally stable.

Consider the one-dimensional advection–diffusion equation

$$\frac{\partial u}{\partial t} + \alpha \frac{\partial u}{\partial x} = \beta \frac{\partial^2 u}{\partial x^2} \quad (x, t) \in [0, L] \times [0, T] \quad (1)$$

with initial conditions

$$u(x, 0) = \phi(x)$$

and boundary conditions

$$u(0, t) = g_0(t), u(L, t) = g_1(t) \quad t \in [0, T]$$

The advection–diffusion equation is significant in physical systems such as fluid dynamics [14–16]. Equation (1) describes partial differential equations in their one-dimensional version, explaining advection–diffusion of quantities such as mass, heat, energy, vorticity. In [17], the impact of different kinds of parameters on velocity and temperature profiles is given, and it was concluded that, in some cases, a boost of volume fraction of nanoparticle led to a decrease in heat transfer rate, and this was a contradiction to the results of other researchers. Influence of viscous dissipation and heat generation/absorption of non-Newtonian power-law fluid is given in [18]. The equations were solved numerically by implementing the Runge–Kutta–Fehlberg fourth-fifth-order method, and results displayed through graphs. The injection parameter escalation was responsible for the decay of the local Nusselt number for both Newtonian and non-Newtonian nanofluid flow. In existing published research, results were obtained, and those results were often displayed in graphs. Thus, in [19], it was mentioned that the performance of heat transfer of non-Newtonian nanofluid was better than that obtained by Newtonian nanofluid for the case of injection and an impermeable plate.

Using the equation in solving systems consists of difficult initials, and boundary conditions provide little or no knowledge regarding analytical solutions [14,20]. However, [21,22] reveal a significant effort to form stable and accurate numerical techniques for the solution of Equation (1). Effects of Endothermic/Exothermic chemical reaction of MHD free convection flow have been studied in [23]. In the presence of a non-uniform heat source/sink, the Carreau nanoparticle is studied by Khan et al. [24]. In this study, in the presence of suction, heat radiation, and a heat source/sink, Jamaludin et al. [25] numerically investigate the stagnant convection mixture-point flow nanofluid over a vertical stretching/shrinking sheet.

On the other hand, compact finite difference schemes can be used to find numerical solutions of differential equations on a smaller number of grid points. An existing scheme was updated [26] to three dimensions for solving the three-dimensional convection–diffusion problem. The scheme was called an exponential higher-order compact finite difference scheme. It provided an exact solution of homogeneous convection–diffusion problems with constant coefficients. A numerical scheme [27] consisted of implicit Euler for time discretization, and hybrid scheme for spatial discretization was studied. Since the solution of the type of equations considered was exhibited as a boundary layer, a piecewise uniform Shishkin mesh was considered for discretization in the spatial direction. A new high-order compact ADI method [28] has been considered for solving the time-dependent convection–diffusion equation. In addition, a correction technique was applied for reducing the error of the splitting term. Two numerical schemes, named the upwind-penalty method and SUPG method, were introduced in [29]. The stability analysis was given, and a comparison with the standard SUPG finite element method was given. Most recent research on the proposed numerical schemes can be found in [30,31].

The proposed compact scheme is constructed on three grid points that can be used to find solutions of convection–diffusion type problems. The scheme is explicit and can be used in some situations to obtain the solution without using the additional iterative scheme to solve discretized/difference equations. The existing corresponding implicit discretization is modified, and so, in this manner, an explicit scheme containing a second-

order partial derivative in time term is obtained. The existing implicit compact scheme consisted of the mixed partial derivative term in space and time, and this term was responsible for establishing an implicit compact scheme rather than an explicit one. In this contribution, however, this mixed derivative term is turned into a second-order partial derivative in time term, and this term is discretized using a second-order standard–classical central difference formula constructed on three time levels. The first-order partial derivative in the time term is discretized using the standard/classical difference formula. The second-order difference formula is used to obtain the second accurate scheme in time and the fourth order in space. This second-order difference formula, however, can be replaced with the first-order difference formula to get the first-order accuracy in the time scheme. However, the fourth-order space accuracy can still be obtained.

Construction of Compact Scheme

Consider the convection–diffusion equation of the form

$$\frac{\partial U}{\partial t} + \frac{\partial U}{\partial x} = \frac{\partial^2 U}{\partial x^2} \tag{2}$$

In the first part of the scheme, Equation (1) is discretized as

$$\frac{u_i^{n+1} - u_i^{n-1}}{2\Delta t} + \frac{u_{i+1}^n - u_{i-1}^n}{2\Delta x} = \frac{u_{i+1}^n - 2u_i^n + u_{i-1}^n}{(\Delta x)^2} \tag{3}$$

Equation (3) is the classical/standard discretization of Equation (2). To use a compact scheme, one remainder term for space discretization of Equation (3) is considered as

$$\frac{u_i^{n+1} - u_i^{n-1}}{2\Delta t} + \frac{u_{i+1}^n - u_{i-1}^n}{2\Delta x} - \frac{(\Delta x)^2}{6} u_{xxx} = \frac{u_{i+1}^n - 2u_i^n + u_{i-1}^n}{(\Delta x)^2} - \frac{(\Delta x)^2}{12} u_{xxxx} \tag{4}$$

Since the third and fourth partial derivatives of u aren't available, these derivatives are found first. Therefore, finding the third and fourth-order derivative of Equation (2) yields

$$\frac{\partial^3 u}{\partial x^3} = \frac{\partial^2 u}{\partial x \partial t} + \frac{\partial^2 u}{\partial x^2} \tag{5}$$

$$\frac{\partial^4 u}{\partial x^4} = \frac{\partial^3 u}{\partial x^2 \partial t} + \frac{\partial^3 u}{\partial x \partial t} + \frac{\partial^2 u}{\partial x^2} \tag{6}$$

Substituting the third- and fourth-order derivative into Equation (4) gives a compact scheme that is implicit. Instead of this, the fourth-order partial derivative in Equation (6) can be expressed as

$$\frac{\partial^4 u}{\partial x^4} = \frac{\partial^2 u}{\partial t^2} + \frac{\partial^2 u}{\partial x \partial t} + \frac{\partial^2 u}{\partial t \partial x} + \frac{\partial^2 u}{\partial x^2} \tag{7}$$

Substituting Equations (5) and (7) into (4) yields

$$\frac{u_i^{n+1} - u_i^{n-1}}{2\Delta t} + \frac{u_{i+1}^n - u_{i-1}^n}{2\Delta x} - \frac{(\Delta x)^2}{6} \left(\frac{\partial^2 u}{\partial x \partial t} + \frac{\partial^2 u}{\partial x^2} \right) = \frac{u_{i+1}^n - 2u_i^n + u_{i-1}^n}{(\Delta x)^2} - \frac{(\Delta x)^2}{12} \left(\frac{\partial^2 u}{\partial t^2} + 2 \frac{\partial^2 u}{\partial t \partial x} + \frac{\partial^2 u}{\partial x^2} \right) \tag{8}$$

Simplifying Equation (8) gives

$$\frac{u_i^{n+1} - u_i^{n-1}}{2\Delta t} + \frac{u_{i+1}^n - u_{i-1}^n}{2\Delta x} - \frac{(\Delta x)^2}{6} \frac{\partial^2 u}{\partial x^2} = \frac{u_{i+1}^n - 2u_i^n + u_{i-1}^n}{(\Delta x)^2} - \frac{(\Delta x)^2}{12} \left(\frac{\partial^2 u}{\partial t^2} + \frac{\partial^2 u}{\partial x^2} \right). \tag{9}$$

In operator form, Equation (9) is expressed as

$$\delta_t u_i^n + \delta_x u_i^n - \frac{(\Delta x)^2}{6} \delta_x^2 u_i^n = \delta_x^2 u_i^n - \frac{(\Delta x)^2}{12} (\delta_t^2 u_i^n + \delta_x^2 u_i^n) \tag{10}$$

where $\delta_t u_i^n = \frac{u_i^{n+1} - u_i^{n-1}}{2\Delta t}$, $\delta_x u_i^n = \frac{u_{i+1}^n - u_{i-1}^n}{2\Delta x}$, $\delta_x^2 u_i^n = \frac{u_{i+1}^n - 2u_i^n + u_{i-1}^n}{(\Delta x)^2}$ and $\delta_t^2 u_i^n = \frac{u_i^{n+1} - 2u_i^n + u_i^{n-1}}{(\Delta t)^2}$.

Equation (10) is an explicit compact difference equation that is fourth order in space and second order in time, and it is constructed on three time levels. Thus, it requires an additional scheme evaluated on the first time level.

2. Stability Analysis

The Von Neumann stability criterion is employed to check the stability of the proposed explicit scheme. According to this criterion, some transformations are considered first as

$$u_i^{n\pm 1} = E^{n\pm 1} e^{iI\phi}, \quad u_{i\pm 1}^n = E^n e^{(i\pm 1)I\phi} \tag{11}$$

Employing transformation (11) into Equation (9) and dividing by $e^{iI\phi}$ gives

$$\begin{aligned} & \frac{E^{n+1} - E^{n-1}}{2\Delta t} + \frac{(e^{I\phi} - e^{-I\phi})E^n}{2\Delta x} - \frac{(\Delta x)^2}{6} \left(\frac{e^{I\phi} - 2 + e^{-I\phi}}{(\Delta x)^2} \right) \\ &= \frac{(e^{I\phi} - 2 + e^{-I\phi})E^n}{(\Delta x)^2} - \frac{(\Delta x)^2}{12} \left(\frac{E^{n+1} - 2E^n + E^{n-1}}{(\Delta t)^2} + \frac{(e^{I\phi} - 2 + e^{-I\phi})E^n}{(\Delta x)^2} \right) \end{aligned} \tag{12}$$

Equation (12) can be expressed as

$$E^{n+1} = AE^n + BE^{n-1} \tag{13}$$

where

$$A = \frac{bd(-6cdI\sin\theta + \Delta td(\cos\theta - 1) + 12d^2(\cos\theta - 1) + 1)}{1 + bd}, \quad B = \frac{1 - \frac{1}{bd}}{1 + \frac{1}{bd}} = \frac{bd - 1}{bd + 1}$$

Since the proposed scheme is constructed on the three time level, it requires one more equation, which can be constructed as

$$E^n = E^n + OE^{n-1}$$

Equations (13) and (14) are expressed as

$$\begin{bmatrix} E^{n+1} \\ E^n \end{bmatrix} = \begin{bmatrix} A & B \\ 1 & 0 \end{bmatrix} \begin{bmatrix} E^n \\ E^{n-1} \end{bmatrix} \tag{14}$$

Here, the amplification factor is a matrix. The eigenvalues of this matrix are used to construct stability conditions that can be expressed as

$$|\lambda_1| \leq 1 \text{ and } |\lambda_2| \leq 1 \left| \frac{A}{2} - \frac{1}{2}\sqrt{A^2 + 4B} \right| \leq 1 \text{ and } \left| \frac{A}{2} + \frac{1}{2}\sqrt{A^2 + 4B} \right| \leq 1 \tag{15}$$

Let $A = A_1 + IB_1$

where

$$A_1 = \Delta td(\cos\phi - 1) + 12d^2(\cos\phi - 1) + 1, \quad B_1 = -2c\sin\phi$$

Let

$$A = A_1 + IB_1 \tag{16}$$

$$A^2 + 4B = A_1^2 - B_1^2 + 2IA_1B_1 + 4B = r(\cos\psi + I\sin\psi)$$

where $r^2 = (A_1^2 - B_1^2 + 4B)^2 + 4A_1^2B_1^2$ and $\psi = \tan^{-1}\left(\frac{2A_1B_1}{A_1^2 - B_1^2 + 4B}\right)$

$$(A^2 + 4B)^{1/2} = r^{1/2} \left(\cos\left(\frac{\psi + 2k\pi}{2}\right) + I\sin\left(\frac{\psi + 2k\pi}{2}\right) \right), \quad k = 0, 1 \tag{17}$$

The condition $\left| \frac{A}{2} - \frac{1}{2}(A^2 + 4B)^{\frac{1}{2}} \right|^2 \leq 1$ implies

$$\left(\frac{A_1}{2} - r^{\frac{1}{2}} \cos\left(\frac{\psi + 2k\pi}{2}\right) \right)^2 + \left(\frac{B_1}{2} + r^{\frac{1}{2}} \sin\left(\frac{\psi + 2k\pi}{2}\right) \right)^2 \leq 1 \tag{18}$$

In addition, the condition $\left| \frac{A}{2} + \frac{1}{2}(A^2 + 4B)^{\frac{1}{2}} \right|^2 \leq 1$ implies

$$\left(\frac{A_1}{2} + r^{\frac{1}{2}} \cos\left(\frac{\psi + 2k\pi}{2}\right) \right)^2 + \left(\frac{B_1}{2} + r^{\frac{1}{2}} \sin\left(\frac{\psi + 2k\pi}{2}\right) \right)^2 \leq 1 \tag{19}$$

Consider the system of convection–diffusion equations

$$\frac{\partial u}{\partial t} + v \frac{\partial u}{\partial y} = \frac{\partial^2 u}{\partial y^2} + a\theta. \tag{20}$$

$$\frac{\partial \theta}{\partial t} + v \frac{\partial \theta}{\partial y} = b \frac{\partial^2 \theta}{\partial y^2} \tag{21}$$

The system of Equations (20) and (21) can be expressed as

$$\bar{A} \frac{\partial \mathbf{U}}{\partial t} + B \frac{\partial \mathbf{U}}{\partial y} = C \frac{\partial^2 \mathbf{U}}{\partial y^2} + D\mathbf{U} \tag{22}$$

where $\bar{A} = \begin{bmatrix} 1 & 0 \\ 0 & 1 \end{bmatrix}$, $B = \begin{bmatrix} v & 0 \\ 0 & v \end{bmatrix}$, $C = \begin{bmatrix} 1 & 0 \\ 0 & b \end{bmatrix}$, $D = \begin{bmatrix} 0 & a \\ 0 & 0 \end{bmatrix}$, $\mathbf{U} = [u, \theta]^t$.

The proposed scheme requires a third- and fourth-order derivative, therefore

$$\frac{\partial^2 \mathbf{U}}{\partial y^2} = C^{-1}(\bar{A}\mathbf{U}_t + B\mathbf{U}_y - D\mathbf{U})\mathbf{U}_{yyy} = C^{-1}(\bar{A}\mathbf{U}_{ty} + b\mathbf{U}_{yy} - D\mathbf{U}_y) \tag{23}$$

$$\begin{aligned} \mathbf{U}_{yyyy} &= C^{-1}(\bar{A}\mathbf{U}_{tyy} + b\mathbf{U}_{yyy} - D\mathbf{U}_{yy}) \\ &= A_1\mathbf{U}_{tt} + A_2\mathbf{U}_{ty} + A_3\mathbf{U}_{yy} - C^{-1}\bar{A}C^{-1}D\mathbf{U}_t - BC^{-1}D\mathbf{U}_y - D\mathbf{U}_{yy} \end{aligned} \tag{24}$$

where $A_1 = C^{-1}\bar{A}C^{-1}\bar{A}$, $A_2 = C^{-1}\bar{A}C^{-1}B + BC^{-1}\bar{A}$ and $A_3 = BC^{-1}B$.

Theorem 1. *The compact scheme for Equation (22) converges subject to the conditions*

- (i) *Error at the first time level is bounded.*
- (ii) $\frac{\bar{A}}{2\Delta t} - \frac{(\Delta y)^2}{6} C^{-1}\bar{A} - \frac{A_2}{\Delta y \Delta t} - \frac{C^{-1}\bar{A}C^{-1}D}{2\Delta t} \geq 0$.

Proof. The compact scheme for Equation (21) is given as

$$\begin{aligned} &\bar{A}\delta_t \mathbf{U}_i^n + B \left(\delta_y \mathbf{U}_i^n - \frac{(\Delta y)^2}{6} (C^{-1}\bar{A}\mathbf{U}_{ty} + C^{-1}B\mathbf{U}_{yy} - C^{-1}D\mathbf{U}_y) \right) \\ &= C \left(\delta_y^2 \mathbf{U}_I^n - \frac{(\Delta y)^2}{12} (A_1\mathbf{U}_{tt} + A_2\mathbf{U}_{ty} + A_3\mathbf{U}_{yy} - C^{-1}\bar{A}C^{-1}D\mathbf{U}_t - BC^{-1}D\mathbf{U}_y - D\mathbf{U}_{yy}) \right) \end{aligned} \tag{25}$$

Let the difference between exact and numerical approximate solution is expressed as $e_i^n = \left| \mathbf{U}_i^n - \bar{\mathbf{U}}_i^n \right|$, where $\bar{\mathbf{U}}_i^n$ shows an exact solution at the i^{th} grid point and at the n^{th} level. The error equation corresponding to Equation (25) is given as

$$\begin{aligned}
 & \left(\frac{e_i^{n+1} - e_i^{n-1}}{2\Delta t} \right) + B \left(\frac{e_{i+1}^n - e_{i-1}^n}{2\Delta y} \right. \\
 & \left. - \frac{(\Delta y)^2}{6} \left(C^{-1} \bar{A} \left\{ \frac{e_{i+1}^{n+1} - e_{i-1}^{n+1}}{2\Delta y \Delta t} - \frac{e_{i+1}^{n-1} - e_{i-1}^{n-1}}{2\Delta y \Delta t} \right\} + C^{-1} B \frac{e_{i+1}^n - 2e_i^n + e_{i-1}^n}{(\Delta y)^2} \right. \right. \\
 & \left. \left. - C^{-1} D \frac{e_{i+1}^n - e_{i-1}^n}{2\Delta y} \right) \right) \\
 & = C \left(\frac{e_{i+1}^n - 2e_i^n + e_{i-1}^n}{(\Delta y)^2} \right) \\
 & - \frac{(\Delta y)^2}{12} \left(A_1 \frac{e_{i+1}^{n+1} - 2e_i^{n+1} + e_{i-1}^{n+1}}{(\Delta t)^2} + A_2 \left(\frac{e_{i+1}^{n+1} - e_{i-1}^{n+1}}{2\Delta y \Delta t} - \frac{e_{i+1}^{n-1} - e_{i-1}^{n-1}}{2\Delta y \Delta t} \right) + A_3 \frac{e_{i+1}^n - 2e_i^n + e_{i-1}^n}{(\Delta y)^2} \right. \\
 & \left. - C^{-1} \bar{A} C^{-1} D \frac{e_{i+1}^{n+1} - e_{i-1}^{n+1}}{2\Delta t} - BC^{-1} D \frac{e_{i+1}^n - e_{i-1}^n}{2\Delta y} - D \frac{e_{i+1}^n - 2e_i^n + e_{i-1}^n}{(\Delta y)^2} \right)
 \end{aligned} \tag{26}$$

Applying norm on both sides of the Equation (26) gives

$$\begin{aligned}
 & \frac{\|\bar{A}\|}{2\Delta t} e^{n+1} \leq \frac{\|\bar{A}\| e^{n-1}}{2\Delta t} + \frac{\|B\| e^n}{2\Delta t} + \frac{(\Delta y)^2}{6} \left(\frac{\|C^{-1} \bar{A}\| e^{n+1}}{\Delta y \Delta t} + \frac{e^{n-1}}{\Delta y \Delta t} \right. \\
 & \left. + \frac{\|C^{-1} B\| 4e^n}{(\Delta y)^2} + \frac{\|C^{-1} D\| e^n}{\Delta y} \right) \\
 & + \|C\| \left(\frac{4e^n}{(\Delta y)^2} + \frac{(\Delta y)^2}{12} \left(\|A_1\| \frac{4e^n}{(\Delta y)^2} + \right. \right. \\
 & \left. \left. \|A_2\| \left(\frac{e^{n+1}}{\Delta y \Delta t} + \frac{e^{n-1}}{\Delta y \Delta t} \right) + \|A_3\| \frac{4e^n}{(\Delta y)^2} + \right. \right. \\
 & \left. \left. \|C^{-1} \bar{A} C^{-1} D\| \frac{e^{n+1} + e^{n-1}}{2\Delta t} + \frac{\|BC^{-1} D\| e^n}{\Delta y} + \frac{\|D\| 4e^n}{(\Delta y)^2} \right) \right)
 \end{aligned} \tag{27}$$

Equation (27) can be expressed as

$$\delta e^{n+1} \leq \delta_1 e^{n-1} + \delta_2 e^n + M \left(O((\Delta t)^2), (\Delta y)^4 \right) \tag{28}$$

where $\delta = \frac{\|A\|}{2\Delta t} - \frac{(\Delta y)^2}{6} \|C\| \left(\frac{\|C^{-1} A\|}{\Delta y \Delta t} - \frac{\|A_2\|}{2\Delta y \Delta t} - \frac{\|C^{-1} A C^{-1} D\|}{4\Delta t} \right)$

$$\begin{aligned}
 \delta_1 & = \|A\| \frac{1}{2\Delta t} + \frac{\Delta y}{6\Delta t} + \frac{(\Delta y)^2}{12} \|C\| \left(\frac{\|A_2\|}{\Delta y \Delta t} + \|C^{-1} \bar{A} C^{-1} D\| \frac{1}{2\Delta t} \right) \\
 \delta_2 & = \frac{\|B\|}{2\Delta x} + \frac{(\Delta y)^2}{6} \left(\|C^{-1} B\| \frac{4}{(\Delta y)^2} + \|C^{-1} D\| \frac{1}{\Delta y} \right) + \|C\| \left(\frac{4}{(\Delta y)^2} + \frac{(\Delta y)^2}{12} \left(\|A_1\| \frac{4}{(\Delta y)^2} + \|A_3\| \frac{4}{(\Delta y)^2} + \right. \right. \\
 & \left. \left. \|BC^{-1} D\| \frac{1}{\Delta y} + \|D\| \frac{4}{(\Delta y)^2} \right) \right)
 \end{aligned}$$

Inequality (28) can be expressed as

$$e^{n+1} \leq \delta_3 e^{n-1} + \delta_4 e^n + M_1 \left(O((\Delta t)^2), (\Delta y)^4 \right) \tag{29}$$

Let $e^{n-1} = \max(e^{n-1}, e^n)$, then Inequality (28) can be expressed as:

$$e^{n+1} \leq \delta_5 e^{n-1} + M_1 \left(O((\Delta t)^2), (\Delta y)^4 \right) \tag{30}$$

Letting $n = 1$ in (30) gives

$$e^2 \leq \delta_5 e^0 + M_1 \tag{31}$$

Since the initial condition is exact, $e^0 = 0$; therefore, (31) becomes

$$e^2 \leq M_1 \tag{32}$$

Letting $n = 2$ in (30) gives

$$e^3 \leq \delta_5 e^1 + M_1 \tag{33}$$

Since the error at first time level is bounded, $e^1 \leq B$; therefore, Equation (33) becomes

$$e^3 \leq \delta_5 B + M_1 \quad (34)$$

Putting $n = 3$ in Equation (30) results in

$$e^4 \leq \delta_5 e^2 + M_1 \leq (\delta_5 + 1)M_1 \quad (35)$$

Putting $n = 4$ in Equation (30) gives

$$e^5 \leq \delta_5 e^3 + M_1 \leq \delta_5^2 B + (\delta_5 + 1)M_1 \quad (36)$$

If it is continued, then for

$$e^{2n+1} \leq \delta_5^n B + (\delta_5^{n-1} + \dots + \delta_5 + 1)M_1. \quad (37)$$

and

$$e^{2n+2} \leq (\delta_5^{n-1} + \dots + \delta_5 + 1)M_1 \quad (38)$$

This implies

$$e^{2n+1} \leq \delta_5^n B + \left(\frac{\delta_5 - 1}{\delta_5 - 1}\right)M_1 \quad (39)$$

and

$$e^{2n+2} \leq \left(\frac{\delta_5 - 1}{\delta_5 - 1}\right)M_1 \quad (40)$$

Since $\dots + \delta_5^{n-1} + \dots + \delta_5 + 1$ is an infinite geometric series, it converges; if $|\delta_5| < 1$ and it gives convergence conditions, then this is the case when $\max(e^n, e^{n-1}) = e^{n-1}$. Similarly, for the case when $\max(e^n, e^{n-1}) = e^n$, the convergence conditions can be found.

The algorithm is constructed that can be used to summarize the use of code for finding the values of unknowns on each grid point and for every time level.

3. Applications

For finding numerical solutions of convection–diffusion problems, two examples are considered. The next part of this contribution comprises the application of the proposed explicit compact scheme for nonlinear PDEs and non-dimensional coupled PDEs for heat transfer in boundary layer flow. An Algorithm 1 is given which summarizes the computer programming for the solution of considered problems.

Algorithm 1. In the beginning, the smallest and largest values of spatial and temporal variables have been defined

Step 1. $\Delta x = (x_1 - x_0)/(N_x - 1)$ and $\Delta t = (t_1 - t_0)/(N_t - 1)$ are the step sizes used in space and time, where N_x and N_t denote grid points and time levels in space and time, respectively, and give values of the parameters contained in the equation(s) considered.

Step 2. Use the forward Euler method on the first time level because the proposed scheme is constructed on three time levels.

Step 3. Use the proposed fourth order in space and second order in time scheme on the remaining time levels to find one unknown explicitly.

Step 4. When values of the dependent variable on each grid point and each time level are computed, a solution can be seen using different plots.

Example 1: Consider the following nonlinear convection–diffusion problem

$$\frac{\partial u}{\partial t} + u \frac{\partial u}{\partial x} = \frac{\partial^2 u}{\partial x^2} \quad (41)$$

subject to the initial and boundary conditions

$$u(x, 0) = 1 - \frac{2}{x}, \quad x > 0 \quad (42)$$

$$u(x_0, t) = 1 - \frac{2}{x_0 - t} \quad \text{and} \quad u(x_1, t) = 1 - \frac{2}{x_1 - t} \quad (43)$$

The exact solution of Equation (41) with initial and boundary conditions (42) and (43), respectively, is given by

$$u(x, t) = 1 - \frac{2}{x - t} \quad (44)$$

The compact discretization for Equation (41) can be expressed as

$$u_i^{n+1} = \left[\begin{array}{l} u_i^{n-1} + \frac{2\Delta t}{(\Delta x)^2} \{ u_{i+1}^n - 2u_i^n + u_{i-1}^n \} - \\ 2\Delta t \left\{ \frac{(\Delta x)^2}{12} \left(\frac{u_i^{n+1} - 2u_i^n + u_i^{n-1}}{(\Delta t)^2} \right) + \right. \\ \left. (u_i^n)^2 \left(\frac{u_{i+1}^n - 2u_i^n + u_{i-1}^n}{(\Delta x)^2} \right) \right\} + \\ 2(\Delta t)u_i^n \left\{ \frac{u_{i+1}^n - u_{i-1}^n}{2\Delta x} + \right. \\ \left. \frac{u_i^n}{6} (u_{i+1}^n - 2u_i^n + u_{i-1}^n) \right\} \end{array} \right] \quad (45)$$

The compact numerical scheme (45) can be changed into an explicit scheme by collecting u_i^{n+1} terms on one side. Thus, in this manner, the second order in time and the fourth order in space scheme for linearized Equation (41) are obtained. Note that the standard/classical second order in the time and space central scheme for Equation (41) becomes unconditionally unstable. Scheme (45), however, which is also second order in time and fourth order in space, becomes conditionally stable. Figure 1a,b show solutions obtained by the proposed scheme and comparisons of exact and standard/classical scheme's solution with one obtained by the proposed scheme. The standard/classical scheme is first order in time and second order in space, and the relative error shown by this scheme is graphed in Figure 1b, which is greater than the relative error obtained by the proposed scheme. N_x and N_t show the number of grid points and time levels, while x_0 and x_1 show the left and right endpoints of the domain.

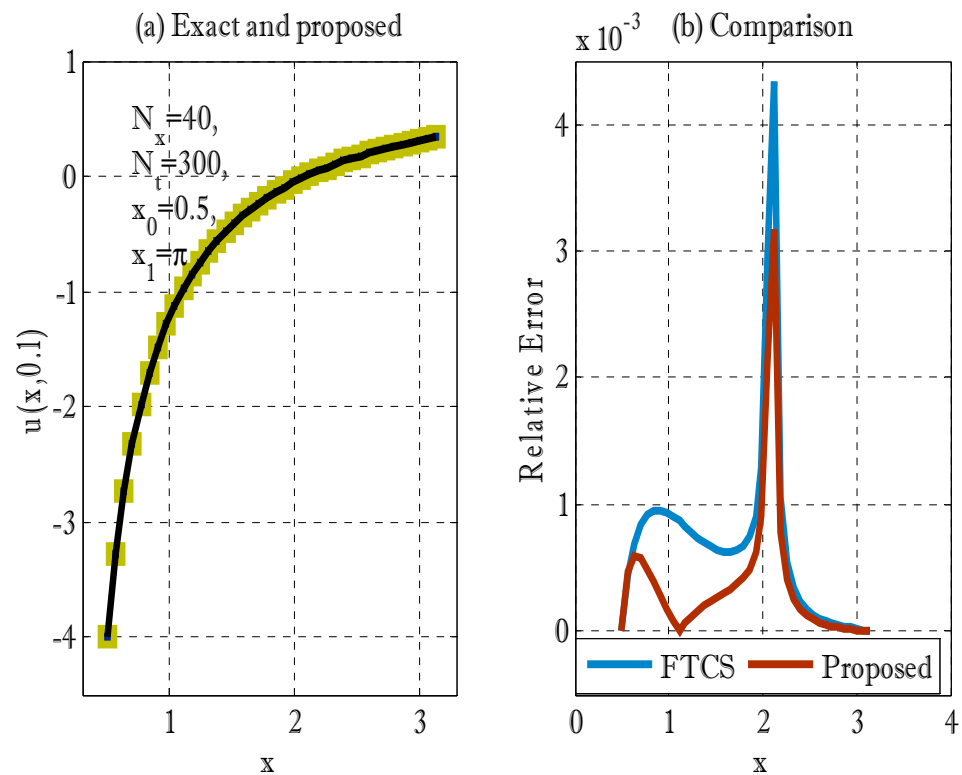


Figure 1. Comparison of the proposed scheme with FTCS. (a) exact and numerical solutions (b) FTCS and proposed schemes.

Example 2: Boundary Layer Flow Over Stretching Sheet

Consider an incompressible, laminar, Newtonian, and two-dimensional unsteady mixed convective fluid flow over an infinitely long plate. Let x^* -axis be along the plate, whereas the y^* -axis is perpendicular to the plate or perpendicular to the direction of the flow. The plate stretches towards the positive x^* -axis and the fluid is placed in the space $y^* > 0$. Let the stretching velocity of the plate be U . Since the plate is infinitely long, the partial derivative in x^* is neglected [23]. Then the governing equations of the flow can be expressed [23] as

$$\frac{\partial v^*}{\partial y^*} = 0 \tag{46}$$

$$\frac{\partial u^*}{\partial t^*} + v^* \frac{\partial u^*}{\partial y^*} = \nu \frac{\partial^2 u^*}{\partial y^{*2}} + g\beta_T(T - T_\infty) \tag{47}$$

$$\frac{\partial T}{\partial t^*} + v^* \frac{\partial T}{\partial y^*} = \alpha \frac{\partial^2 T}{\partial y^{*2}} + \frac{1}{\rho c_p} \frac{\partial q_r}{\partial y^*} \tag{48}$$

subject to the boundary conditions given as

$$\left. \begin{aligned} u^*(y^*, t^*) &= U, T(y^*, t^*) = T_w \text{ when } y^* \rightarrow 0 \\ u^*(y^*, t^*) &= 0, T(y^*, t^*) = T_\infty \text{ when } y^* \rightarrow \infty \end{aligned} \right\} \tag{49}$$

where q_r is the heat flux and u^* and v^* represent the components of velocity in x^* and y^* directions, respectively; ν represents the kinematic viscosity, g is used for gravity, β_T represents the coefficient of volume expansion for temperature, T is the fluid temperature, α represents thermal diffusivity, T_w represents the temperature of the fluid at the wall, and T_∞ represents the temperature of the fluid away from the plate.

Equations (46)–(49) are dimensional, so to reduce these equations into dimensionless forms, the following transformations are given as

$$u = \frac{u^*}{U}, V = \frac{v^*}{U}, t = \frac{t^*U^2}{\nu}, y = \frac{Uy^*}{\nu}, \theta = \frac{T - T_\infty}{T_w - T_\infty} \tag{50}$$

Substituting transformations (50) into Equations (46)–(49), the dimensionless equations are given as

$$\frac{\partial v}{\partial y} = 0 \tag{51}$$

$$\frac{\partial u}{\partial t} + v \frac{\partial u}{\partial y} = \frac{\partial^2 u}{\partial y^2} + \frac{Gr_L}{Re^3} \theta \tag{52}$$

$$\frac{\partial \theta}{\partial t} + v \frac{\partial \theta}{\partial y} = \frac{1}{Pr} \left(1 + \frac{4}{3} R_d \right) \frac{\partial^2 \theta}{\partial y^2}. \tag{53}$$

subject to the dimensionless boundary conditions

$$\left. \begin{aligned} u(y, t) = 1, \theta(y, t) = 1 \text{ when } y \rightarrow 0 \\ u(y, t) = 0, \theta(y, t) = 0 \text{ when } y \rightarrow \infty \end{aligned} \right\} \tag{54}$$

where Gr_L represents Grashoff number of heat transfer, R_d is the radiation parameter, Re represents the Reynolds number, and Pr represents the Prandtl number; these parameters are defined by

$$Gr_L = \frac{g\beta_T(T_w - T_\infty)L^3}{\nu^2}, R_d = \frac{4\sigma T_\infty^3}{kk^*}, Re = \frac{\nu}{UL} \text{ and } Pr = \frac{\nu}{\alpha} \tag{55}$$

where σ and k and k^* are, respectively, the Stefan–Boltzmann constant, the thermal conductivity of the fluid, and mean absorption coefficient, and parameters have appeared where radiation parameter R_d was defined in (54). Additionally, in Equation (53), linearized Rosseland radiative flux is considered. The solution of Equation (51) is expressed by

$$v = v_0 \tag{56}$$

where v_0 is suction/injection velocity of the plate.

For solving convection–diffusion type Equations (52)–(53) using the proposed scheme, a difference/discretized equation can be developed in the following manner,

$$u_i^{n+1} = \left[\begin{aligned} & u_i^{n-1} - \frac{V\Delta t}{\Delta y} (u_{i+1}^n - u_{i-1}^n) + \\ & 2\Delta t \left(\frac{(V\Delta y)^2}{12} + 1 \right) \left(\frac{u_{i+1}^n - 2u_i^n + u_{i-1}^n}{(\Delta y)^2} \right) + \\ & \Delta t \left(-\frac{VN(\Delta y)^2}{12} \right) \left(\frac{\theta_{i+1}^n - \theta_{i-1}^n}{2\Delta y} \right) - \\ & \Delta t \left(\frac{(\Delta y)^2}{6} \right) \left(\frac{u_i^{n+1} - 2u_i^n + u_i^{n-1}}{(\Delta t)^2} \right) + \\ & \Delta t \left(\frac{N(\Delta y)^2}{6} \right) \left(\frac{\theta_i^{n+1} - \theta_i^{n-1}}{2\Delta t} \right) \\ & \Delta t \left(\frac{N}{6} \right) (\theta_{i+1}^n - 2\theta_i^n + \theta_{i-1}^n) + \\ & 2\Delta t N \theta_i^n \end{aligned} \right] \tag{57}$$

$$\theta_i^{n+1} = \left[\begin{aligned} & \theta_i^{n-1} - \frac{V\Delta t}{\Delta x} (\theta_{i+1}^n - \theta_{i-1}^n) + \\ & 2\Delta t \left(\frac{(V\Delta x)^2}{12a} + a \right) \left(\frac{\theta_{i+1}^n - 2\theta_i^n + \theta_{i-1}^n}{(\Delta x)^2} \right) - \\ & \Delta t \left(\frac{(\Delta x)^2}{6a} \right) \left(\frac{u_i^{n+1} - 2u_i^n + u_i^{n-1}}{(\Delta t)^2} \right) \end{aligned} \right] \tag{58}$$

where $a = \frac{1}{Pr} \left(1 + \frac{4R_d}{3}\right)$ and $N = \frac{Gr_L}{R_c^3}$. Since the term contained in Eq. (58), having the form θ_i^{n+1} , which is computed from Equation (57). Thus, two different procedures can be adopted. The one using some iteration scheme and this is an implicit kind of procedure to find the values of unknowns, or another one is an explicit procedure that finds θ_i^{n+1} first and afterward, the term u_i^{n+1} is calculated. In this contribution, an explicit procedure is adopted. Some results are compared with existing schemes. Figure 2 shows the solution obtained by the proposed scheme with the exact solution and two existing schemes. The comparison with the exact solution is given in Figure 2a, while the comparison of absolute errors made by three schemes is drawn in Figure 2b. The proposed scheme produced less error than the first order in time and second order in space scheme, and the absolute error obtained by the DuFort–Frankel method oscillates. Figure 3 shows the comparison of the proposed scheme with the DuFort–Frankel scheme through time. Skin friction coefficient starts with zero due to an initial condition is set to zero, and then for the next time level, it starts with its highest value. Then it decreases and maintains an approximately/exactly constant behavior along the x -axis. The difference between skin friction coefficients obtained by both schemes can be seen in the zoomed figure. In addition, it can be observed that the skin friction coefficient oscillates, which is computed from the existing unconditionally stable DuFort–Frankel method. The difference between two local Nusselt numbers obtained by the proposed and existing schemes can be seen in Figure 4. The skin friction coefficient and local Nusselt number decrease over time due to the effects of applied boundary conditions on velocity and temperature profiles, and this effect decreases with time. Figures 5–9 show contour plots for velocity profile for only the diffusion parabolic equation with diffusion effect, including the source term and convection–diffusion equations. The mesh plots, Figures 9 and 10, show the surface type of plot that can be used to understand the contour plots. The symbol x_0 is used left end point of domain, x_1 is used for right end point of domain, t_f is used for final time, N_y is used for number of grid points and N_t is used for number of time levels.

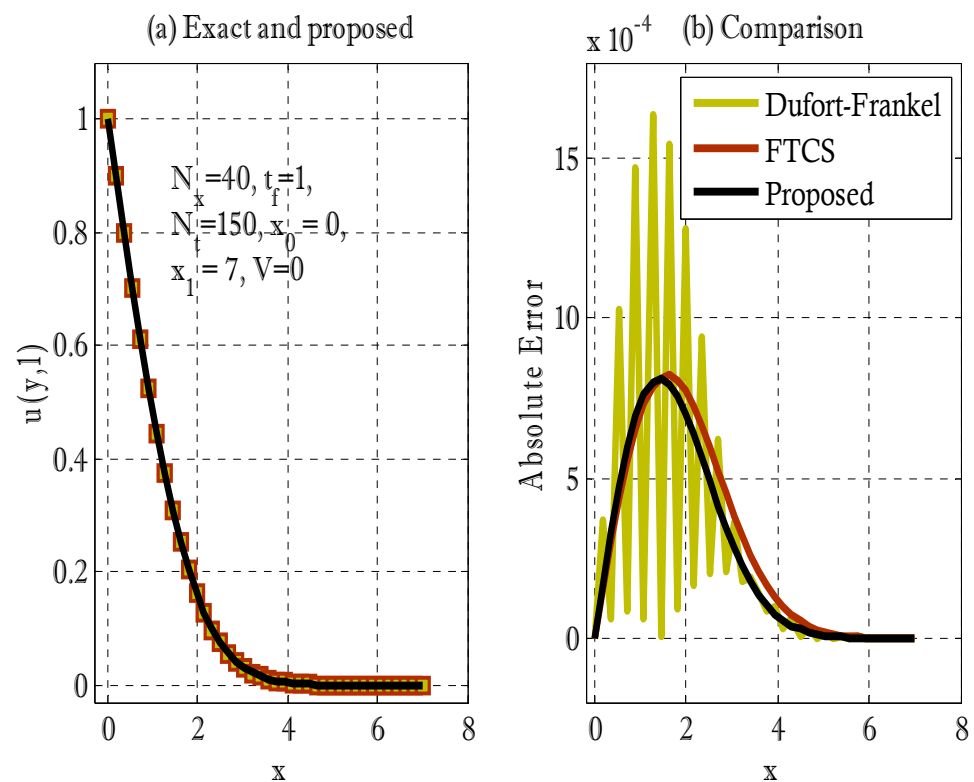


Figure 2. Comparison of the proposed scheme with the FTCS and Dufort–Frankel methods.

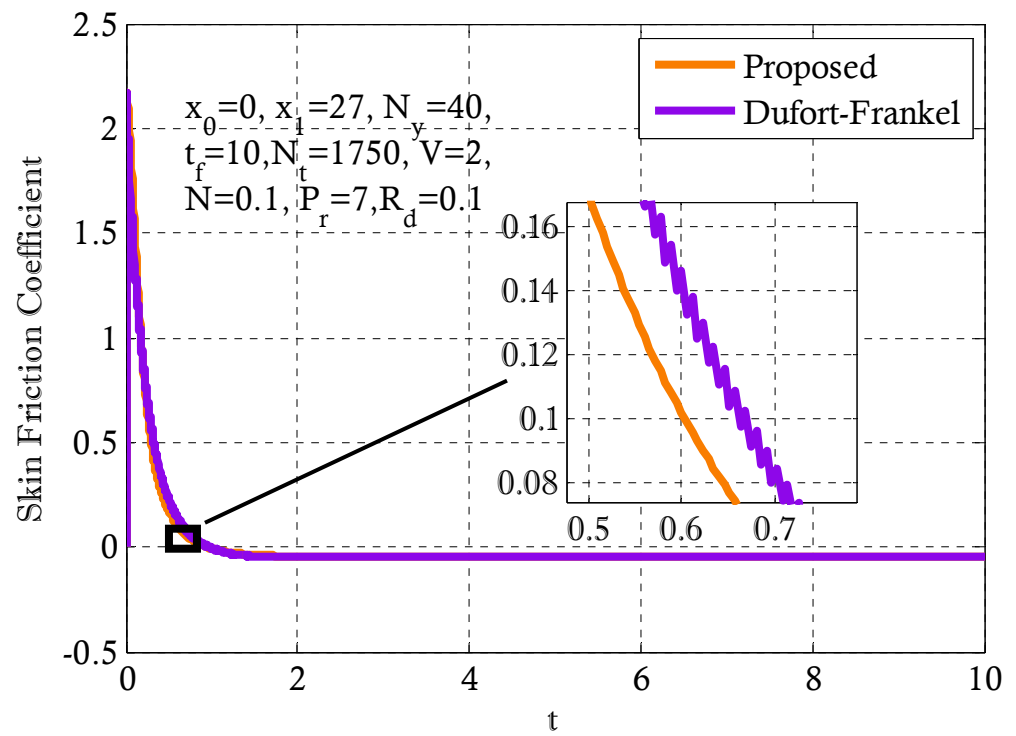


Figure 3. Comparison of the proposed scheme with the Dufort–Frankel method in finding the skin friction coefficient through time.

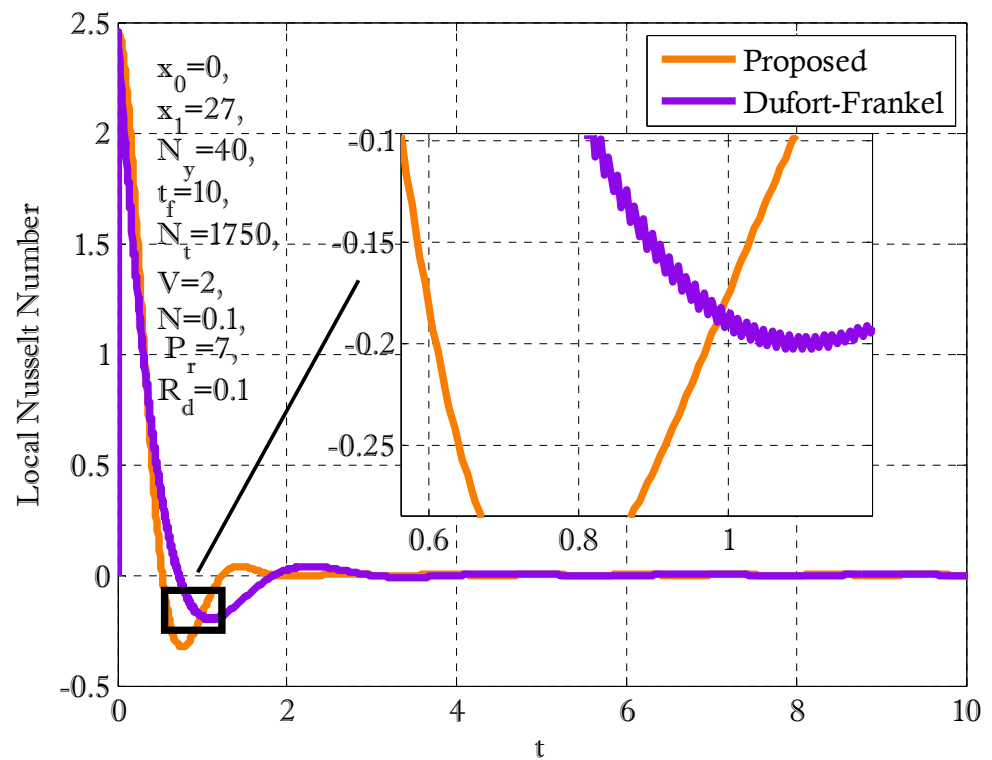


Figure 4. Comparison of the proposed scheme with the Dufort–Frankel method in finding the local Nusselt number through time.

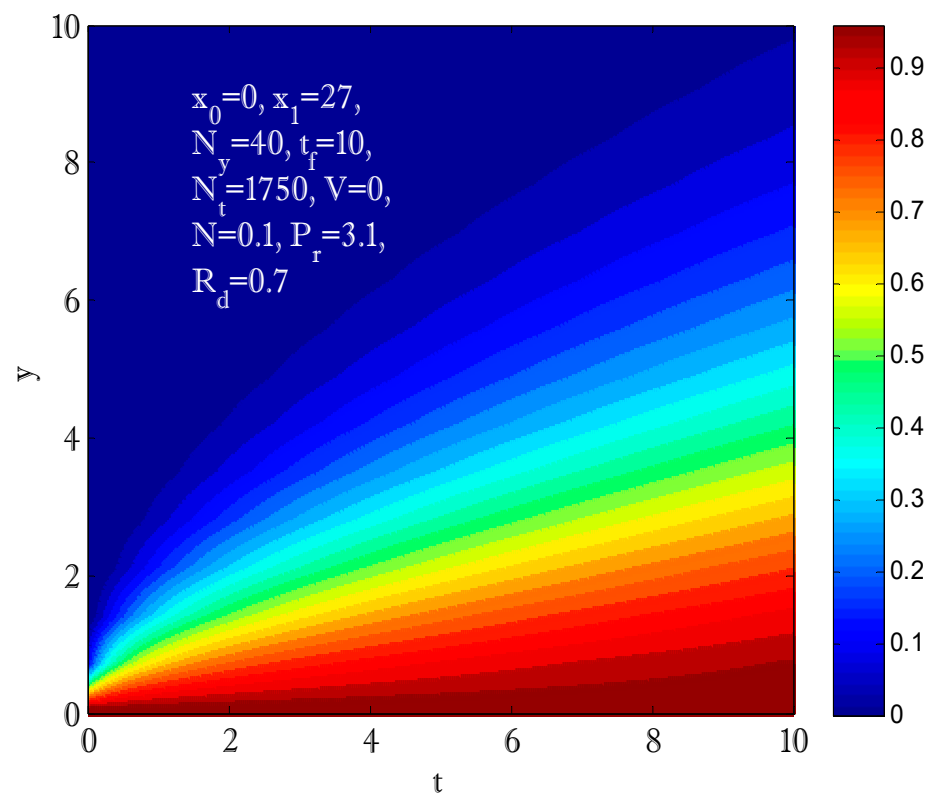


Figure 5. Contour plot for velocity using $V = 0$.

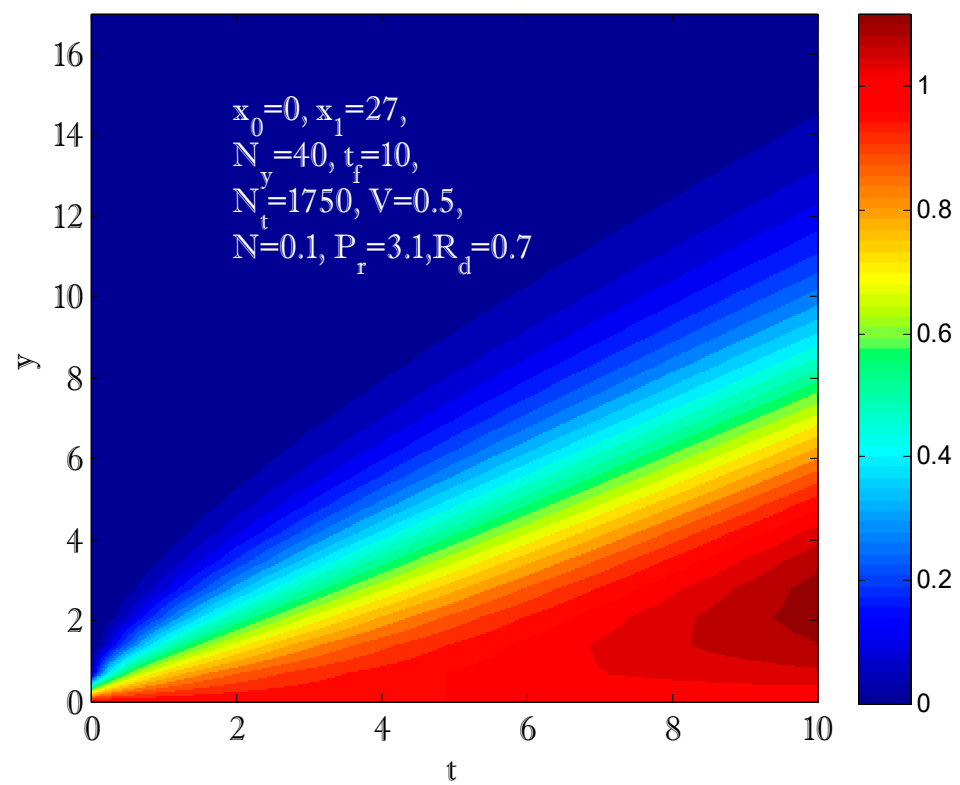


Figure 6. Contour plot for velocity using $V = 0.5$.

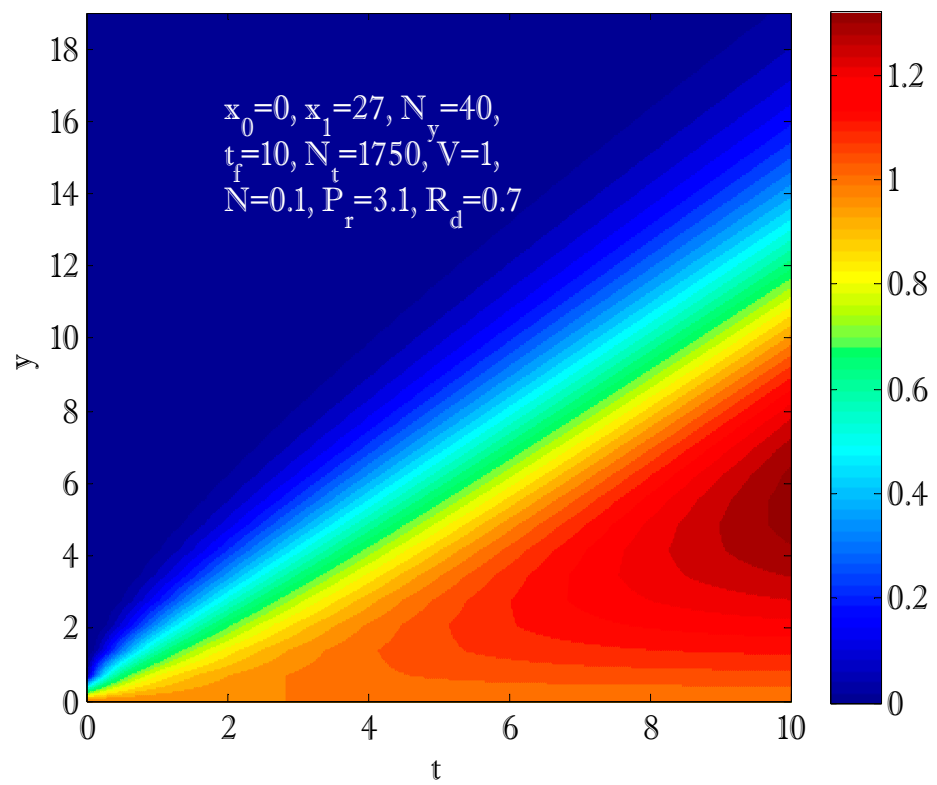


Figure 7. Contour plot for velocity using $V = 1$.

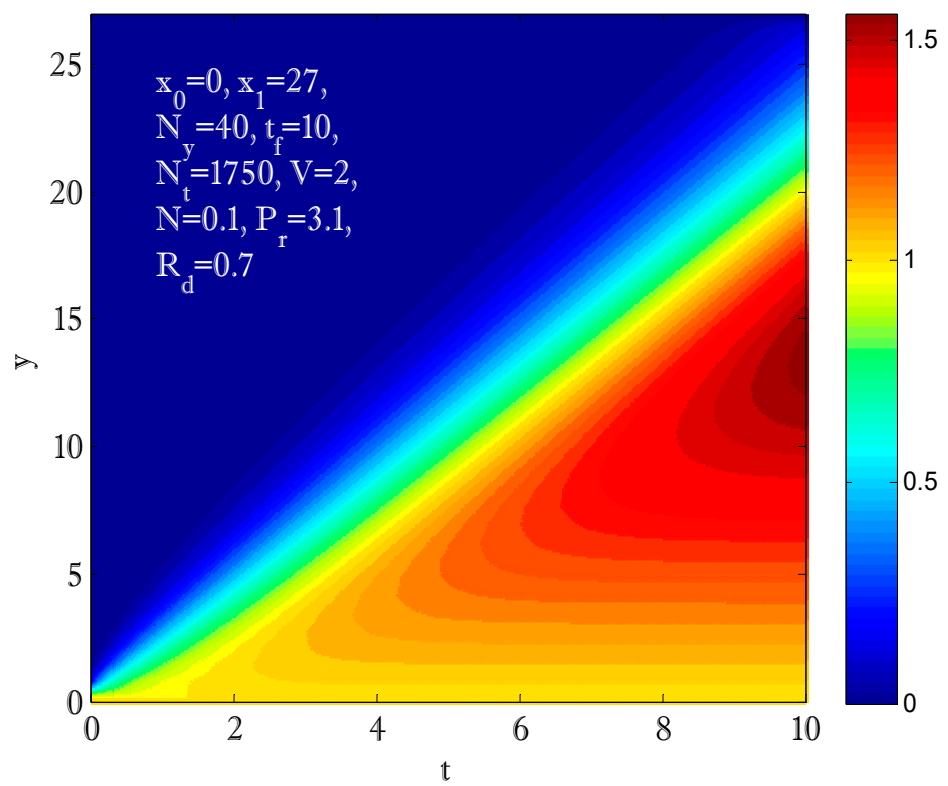


Figure 8. Contour plot for velocity using $V = 2$.

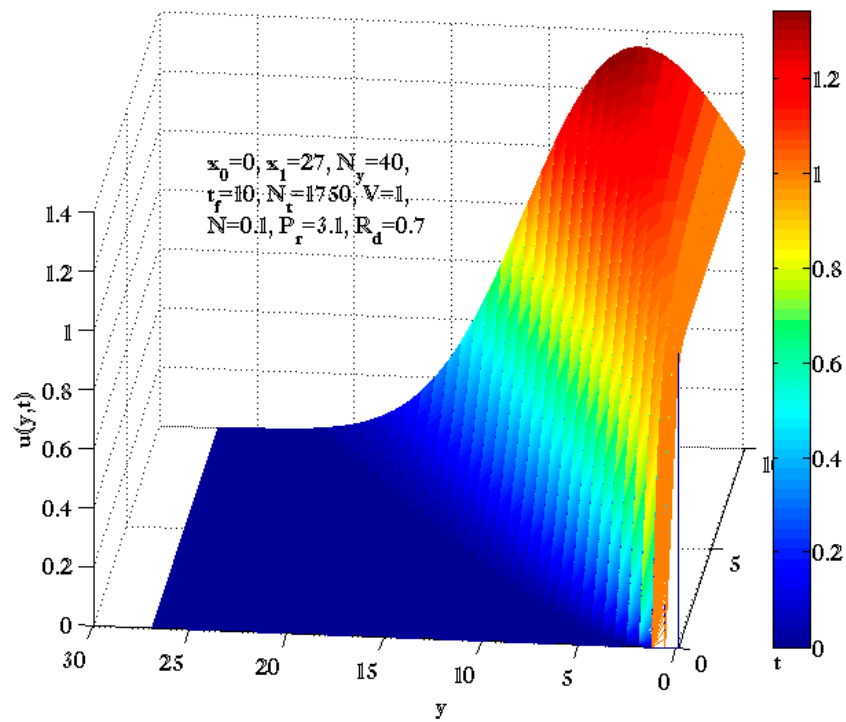


Figure 9. Mesh plot for velocity profile using $V = 1$.

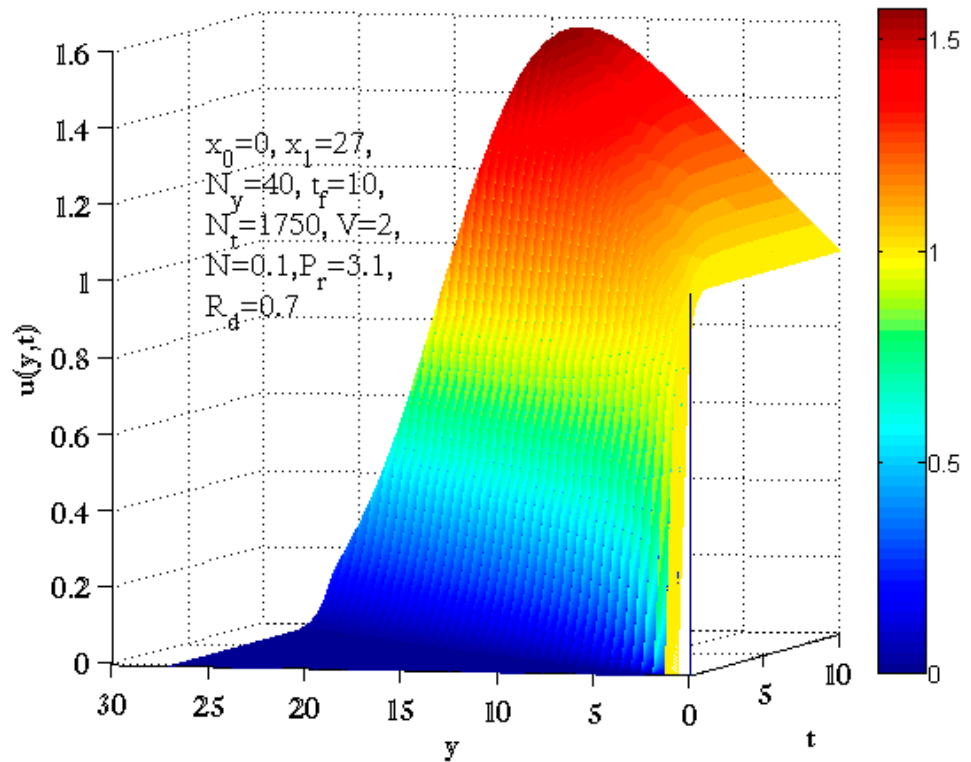


Figure 10. Mesh plot for velocity profile using $V = 2$.

4. Conclusions

A fourth-order explicit compact numerical scheme was proposed for solving convection–diffusion equations. The stability for the scalar case and convergence for the system of partial differential equations were given. A particular case of the existing mathematical model for the heat transfer in mixed convection fluid flow over a stretching sheet with

the influence of thermal radiations was given. The proposed compact numerical scheme was used to solve the dimensionless equations in fluid phenomena with heat transfer effects, and some results were compared with existing schemes. It is hoped that the results in the current report are a helpful source for future fluid-flow studies in an industrial environment in an enclosure area.

Author Contributions: Conceptualization, methodology, and analysis, Y.N.; funding acquisition, W.S.; investigation, Y.N.; methodology, M.S.A.; project administration, W.S.; resources, W.S.; supervision, M.S.A.; visualization, W.S.; writing—review and editing, M.S.A.; proofreading and editing, A.N. All authors have read and agreed to the published version of the manuscript.

Funding: This research was funded by Prince Sultan University, grant number RG-DES-2017-01-17 and “The APC was funded by Prince Sultan University”.

Institutional Review Board Statement: Not applicable.

Informed Consent Statement: Not applicable.

Data Availability Statement: The manuscript included all required data and information for its implementation.

Acknowledgments: We always thank anonymous referees warmly. We are also very thankful for providing an excellent study atmosphere and infrastructure for the Vice-Chancellor of Islamabad Air University. The third author also thanks Prince Sultan University for funding this research.

Conflicts of Interest: The authors declare no conflict of interest.

References

- Berryman, J.G.; Holland, C.J. Nonlinear diffusion problem arising in plasma physics. *Phys. Rev. Lett.* **1978**, *40*, 1720–1722. [[CrossRef](#)]
- Bertsch, M. Asymptotic behavior of solutions of a nonlinear diffusion equation. *SIAM J. Appl. Math.* **1982**, *42*, 66–76. [[CrossRef](#)]
- Do, H.; Owida, A.A.; Yang, W.; Morsi, Y.S. Numerical simulation of the haemodynamics in end-to-side anastomoses. *Int. J. Numer. Methods Fluids* **2011**, *67*, 638–650. [[CrossRef](#)]
- Bodnar, T.; Sequeira, A. Numerical Simulation of the Coagulation Dynamics of Blood. *Comput. Math. Methods Med.* **2008**, *9*, 83–104. [[CrossRef](#)]
- Black, F.; Scholes, M. The Pricing of Options and Corporate Liabilities. *J. Political Econ.* **1973**, *81*, 637–659. [[CrossRef](#)]
- Merton, R.C. Theory of Rational Option Pricing. *Bell J. Econ.* **1973**, *4*, 141–183. [[CrossRef](#)]
- Seydel, R. *Tools for Computational Finance*, 5th ed.; Springer: London, UK, 2012.
- Ehrhardt, M.; Mickens, R.E. A fast, stable and accurate numerical method for the Black–Scholes equation of American options. *Int. J. Theor. Appl. Fin.* **2008**, *11*, 471–501. [[CrossRef](#)]
- Ehrhardt, M.; Mickens, R.E. A nonstandard finite difference scheme for convection–diffusion equations having constant coefficients. *Appl. Math. Comput.* **2013**, *219*, 6591–6604. [[CrossRef](#)]
- Macias, D.J.E.; Puri, A. An explicit positivity-preserving finite-difference scheme for the classical Fisher–Kolmogorov–Petrovsky–Piscounov equation. *Appl. Math. Comput.* **2012**, *218*, 5829–5837.
- Sun, H.; Zhang, J.A. A high-order compact boundary value method for solving one-dimensional heat equations. *Numer. Methods Part. Differ. Equ.* **2003**, *19*, 846–857. [[CrossRef](#)]
- Mohebbi, A.; Dehghan, M. High-order compact solution of the one-dimensional heat and advection–diffusion equations. *Appl. Math. Model.* **2010**, *34*, 3071–3084. [[CrossRef](#)]
- Noye, B.J. A new third-order finite-difference method for transient one-dimensional advection–diffusion. *Commun. Appl. Numer. Methods* **1990**, *6*, 279–288. [[CrossRef](#)]
- Dehghan, M. Weighted finite difference techniques for the one-dimensional advection–diffusion equation. *Appl. Math. Comput.* **2004**, *147*, 307–319. [[CrossRef](#)]
- Roache, P. *Computational Fluid Dynamics*; Hermosa Press: Albuquerque, NM, USA, 1972.
- Spalding, D.B. A novel finite difference formulation for differential expressions involving both first and second derivatives. *Int. J. Numer. Methods Eng.* **1972**, *4*, 551–559. [[CrossRef](#)]
- Maleki, H.; Alsarrad, J.; Moghanizadeh, A.; Hajabdollahi, H.; Safaei, M.R. Heat transfer and nanofluid flow over a porous plate with radiation and slip boundary conditions. *J. Cent. South Univ.* **2019**, *26*, 1099–1115. [[CrossRef](#)]
- Maleki, H.; Safaei, M.R.; Togun, H.; Mahidzal, D. Heat transfer and fluid flow of pseudo-plastic nanofluid over a moving permeable plate with viscous dissipation and heat absorption/generation. *J. Therm. Anal. Calorim.* **2019**, *135*, 1643–1654. [[CrossRef](#)]

19. Maleki, H.; Safaei, M.R.; Alrashed, A.A.A.A.; Alibakhsh, N. Flow and heat transfer in non-Newtonian nanofluids over porous surfaces. *J. Therm. Anal. Calorim.* **2019**, *135*, 1655–1666. [[CrossRef](#)]
20. Dehghan, M. Numerical solution of the three-dimensional advection–diffusion equation. *Appl. Math. Comput.* **2004**, *150*, 5–19. [[CrossRef](#)]
21. Karahan, H. Unconditional stable explicit finite difference technique for the advection–diffusion equation using spreadsheets. *Adv. Eng. Softw.* **2007**, *38*, 80–86. [[CrossRef](#)]
22. Karahan, H. Implicit finite difference techniques for the advection–diffusion equation using spreadsheets. *Adv. Eng. Softw.* **2006**, *37*, 601–608. [[CrossRef](#)]
23. Abdul, M.K.H. Effects of Exothermic/Endothermic Chemical Reactions with Arrhenius Activation Energy on MHD Free Convection and Mass Transfer Flow in Presence of Thermal Radiation. *J. Thermodyn.* **2013**, 1–11.
24. Khan, N.S.; Gul, T.; Kumam, P.; Shah, Z.; Islam, S.; Khan, W.; Zuhra, S.; Sohail, A. Influence of Inclined Magnetic Field on Carreau Nano liquid Thin Film Flow and Heat Transfer with Graphene Nanop articles. *Energies* **2019**, *12*, 1459. [[CrossRef](#)]
25. Jamaludin, A.; Nazar, R.; Pop, I. Mixed convection stagnation-point flow of a nanofluid past a permeable stretching/shrinking sheet in the presence of thermal radiation and heat source/sink. *Energies* **2019**, *12*, 788. [[CrossRef](#)]
26. Mohamed, N.; Mohamed, S.A.; Seddek, L.F. Exponential higher-order compact scheme for 3D steady convection–diffusion problem. *Appl. Math. Comput.* **2014**, *232*, 1046–1061. [[CrossRef](#)]
27. Das, A.; Natesan, S. Uniformly convergent hybrid numerical scheme for singularly perturbed delay parabolic convection–diffusion problems on Shishkin mesh. *Appl. Math. Comput.* **2015**, *271*, 168–186. [[CrossRef](#)]
28. Wang, K.; Wang, H. Stability and error estimates of a new high-order compact ADI method for the unsteady 3D convection–diffusion equation. *Appl. Math. Comput.* **2018**, *331*, 140–159. [[CrossRef](#)]
29. Jeon, Y. Hybridized SUPG and Upwind numerical schemes for convection dominated diffusion problems. *J. Comput. Appl. Math.* **2015**, *275*, 91–99. [[CrossRef](#)]
30. Nawaz, Y.; Arif, M.S. Modified Class of Explicit and Enhanced Stability Region Schemes: Application to Mixed Convection Flow in a Square Cavity with a Convective Wall. *Int. J. Numer. Methods Fluids* **2021**, *93*, 1759–1787. [[CrossRef](#)]
31. Pasha, A.S.; Nawaz, Y.; Arif, S.M. A third-order accurate in time method for boundary layer flow problems. *Appl. Numer. Math.* **2021**, *161*, 13–26. [[CrossRef](#)]